Schweizerische Eidgenossenschaft
Confédération suisse
Confederazione Svizzera
Confederaziun svizra

Federal Department of the Environment, Transport, Energy and Communications DETEC

Swiss Federal Office of Energy SFOE
Energy Research and Cleantech Division

Final report dated 13th November 2021

Comparative simulation study of lean burn versus stoichiometric operation with EGR for a hydrogen heavy duty combustion engine

---

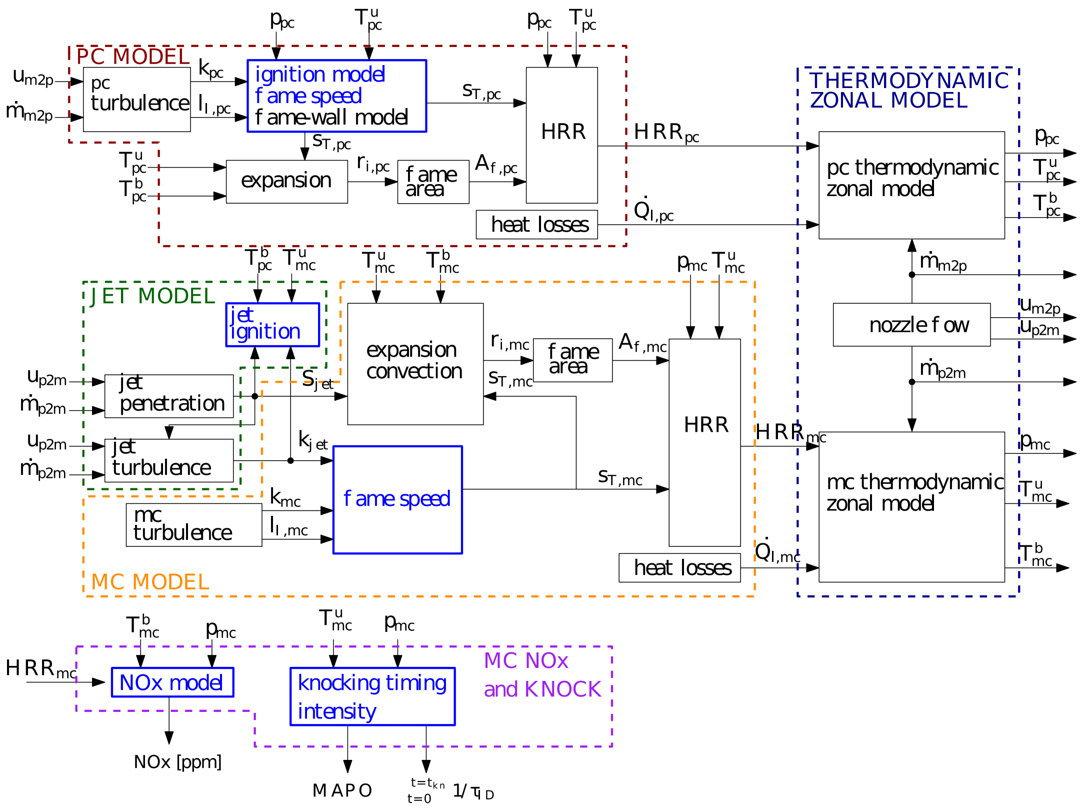

Source: © LAV, ETH Zurich, 2021

Date: 13th November 2021

Location: Bern

Publisher:
Swiss Federal Office of Energy SFOE
Energy Research and Cleantech
CH-3003 Bern
www.bfe.admin.ch

Subsidy recipients:
ETH Zürich
Institut für Energietechnik
Laboratorium für Aerothermochemie und Verbrennungssysteme
Sonneggstrasse 3
CH-8092 Zürich http://www.lav.ethz.ch/

Authors:
Dr. Konstantinos Bardis, Aerothermochemistry and Combustion Systems Laboratory,
ETH Zürich, kbardis@ethz.ch
Prof. Konstantinos Boulouchos, Aerothermochemistry and Combustion Systems Laboratory,
ETH Zürich, kboulouchos@ethz.ch

SFOE project coordinators:
Stephan Renz, info@renzconsulting.ch
Dr. Carina Alles, Carina.Alles@bfe.admin.ch

SFOE contract number: SI/502082

Zusammenfassung

Das vorliegende Projekt beinhaltet eine Simulationsstudie zur Potentialabschätzung eines stationär laufenden wasserstoffbetriebenen Motors für Schwerlast Anwendungen basierend auf einem Gasmotor der Firma Liebherr mit 20 Zylindern und 1MW$_{el}$-Leistung. Die Simulation stützt sich auf ein GT-Power Model dieses Motors, wobei die Verbrennung sowohl mit Vorkammer – als auch mit konventioneller Zündung auf Basis eines an der ETH entwickelten Models (Diss. K. Bardis, 2020) simuliert wird.

Die Simulationsergebnisse für Methan als Brennstoff und Magerbetrieb wurden mit experimentellen Ergebnissen validiert und die Übereinstimmung war sehr gut. Untersucht wurde anschliessend der Betrieb mit Methan als Magermotor und in stöchiometrischer Ausführung mit AGR, sowie der H_2-betriebene Motor ebenfalls eine Mager- und lamda=1+AGR Ausführung. Auf Grund der eingeschränkten Laufzeit des Projektes wurde der Vergleich jeweils an den geschätzten Magerlauf- und Verdünnungsgrenzen (mit AGR) durchgeführt, welche für die beiden Brennstoffe unterschiedlich sind. Ebenfalls wurde das Verdichtungs-Verhältnis des ursprünglichen Motors für alle Fälle beibehalten.

Als Hauptsteuerungsparameter für die Leistung des Motors wurde der Zündzeitpunkt definiert, welcher breit variiert wurde. Als Performance-Kriterien (bei gleichbleibender Leistung von 1MWel entsprechend einem effektiven Mitteldruck von 17bar bei 1'500U/min) wurden der effektive Wirkungsgrad und die NO_x-Emissionen gewählt, wobei als zusätzlich einzuhaltende Randbedingungen der maximale Zylinderdruck, das Druckverhältnis am Verdichter des Turboladers, die Abgastemperatur vor Turbineneintritt und die Klopfgrenze herangezogen wurden. Aus den genannten zeitlichen Gründen wurde nur der «perfekt» homogene Betrieb mit Eindüsung des Brennstoffs vor dem Einlassventil, berücksichtigt. Folgende Ergebnisse wurden unter Einhaltung aller kritischen Randbedingungen generiert:

Für den Betrieb mit Methan ergaben sich maximale Wirkungsgrade von 38,5% für den AGR-Bereich unter Einhaltung der NO_x-Grenze von 100mg/Nm3 @ 5% O_2 und 42% bzw. 39% für den Magerbetrieb ohne bzw. mit Einhaltung dieser NO_x-Grenze (Annahme einer Katalysator-NO_x-Konversion für den AGR Betrieb). Für den Betrieb mit Wasserstoff ergeben sich innerhalb der Rechen- und Annahmegenauigkeiten absolut ähnliche Werte, allerdings:

- Bei der hier betrachteten Eindüsung im Einlass übersteigt das notwendige Druckverhältnis am Verdichter den Wert von 4.5, wodurch eine einstufige Aufladung für das Erreichen der vorgegebenen Leistung von 1MWel wahrscheinlich nicht ausreichen würde.

- Auf Grund der viel höheren Flammgeschwindigkeit von Wasserstoff und der damit verbundenen Brenndauer liegt der optimale Zündzeitpunkt für H_2 deutlich später als derjenige für Methan, dies insbesondere für den stöchiometrischen Betrieb mit AGR.

Die erwähnten Simulationsergebnisse für Wasserstoff gelten jedoch unter dem Vorbehalt der experimentellen Überprüfung gewisser Annahmen in Zusammenhang mit:

- Der Tendenz zur Selbstzündung auf Grund der minimalen Zündenergie von H_2 und somit des Einflusses von heissen Oberflächen im Brennraum.

- Den potentiell höheren Wandwärmeverlusten beim Betrieb mit Wasserstoff auf Grund des erwarteten kleineren Löschabstandes der Flammen von der Brennraumwand.

- Gewisser Unsicherheiten in Zusammenhang mit dem effektiven Wert der laminaren Flammgeschwindigkeit von H_2-Luft-Gemischen bei motorrelevanten Drücken und Temperaturen.

Es scheint deswegen als sinnvoll, diese ersten Erkenntnisse durch nachfolgende experimentelle Projekte, sowohl im Grundlagenbereich als auch durch Messungen am Vollmotor zu ergänzen und zu untermauern. Dies gilt insbesondere für die Anwendung der direkten H_2-Eindüsung im Vergleich zur indirekten.

Summary

A simulation study has been performed in order to evaluate the performance of a stationary $1MW_{el}$-internal combustion engine for heavy duty applications fuelled with hydrogen in comparison to the same engine fuelled with methane. Two operating modes for each fuel have been considered, namely first at the lean burn limit and second with stoichiometric mixtures and at the dilution limit with Exhaust Gas Recirculation (EGR).

This comparative evaluation employed a GT-Power model for the flow and thermodynamic process, complemented by a phenomenological model to describe in detail the power cycle (including combustion) with both pre-chamber (PC) and open-chamber (OC) ignition, which was developed in LAV, ETH (Diss. K. Bardis, 2020). The main criterion of performance is the net thermodynamic efficiency achieved by the engine at each operating mode and with each fuel, while respecting important boundary conditions and operating limits such as the peak cylinder pressure, the burnt gas temperature at the exhaust turbine inlet, the avoidance of knock, the maximal pressure ratio across the compressor as well as different NO_x-limits according to the actual legislation.

The developed pre-chamber combustion model has shown very good agreement with the experimental results in the methane lean-burn mode. Due to the absence of experimental data for the hydrogen operation it was not possible to validate the model with this fuel. Nonetheless, the simulation of methane lean vs. stoichiometric operation with EGR yields consistent trends when compared against previous experimental studies [22] for heavy duty engines. More precisely, the unconstrained efficiency (without the NO_x limit) of methane lean operation is more than 3% (absolute points) higher in comparison to the EGR operation. However, similar efficiency is attained, 39% for the methane lean and 38.5 % for the stoichiometric operation with EGR, respectively, when the NO_x limit of 100mg/Nm3 is considered.

When respecting the various limitation, hydrogen operation shows very similar efficiency with the methane operation. One exception is the hydrogen lean operation with open-chamber where the increased NO_x emission require a delayed spark timing in comparison to the optimal.

Lean burn operation with H_2 and port fuel injection will probably make a 2-stage turbocharger necessary for achieving the required high power densities in the order of a brake mean effective pressure of 17 bar. In contrast, for stoichiometric operation with EGR a single-stage turbo charger is sufficient. The efficiency achieved is relatively high efficiency (37.8% for open-chamber and 39% for prechamber operation) due to the reduced pumping losses in comparison to hydrogen lean operation and the employment of a near optimal spark timing.

The present study constitutes an important step towards the development of hydrogen heavy duty combustion engines and the feasibility of lambda = 1 + EGR operation in comparison to the commonly employed lean burn combustion. Certain key modelling assumptions need to be critically revised in the future and the model needs to be validated extensively once experimental data become available.

Main findings

- Development of a hydrogen and methane phenomenological combustion model including submodels for knocking intensity and NO_x emission; integration of the model in an 1-D commercial simulation software for connection with gas dynamics and turbocharger.

- Comparison of methane lean against stoichiometric operation with EGR confirms previously experimentally observed trends, in which the lean burn operation has higher efficiency (without the NO_x limitation) but similar efficiency to the lambda = 1 + EGR when NO_x emissions are limited by the legislation.

- Lean hydrogen operation with port fuel injection necessitates for a two stage turbocharger to achieve the power density of the methane lean burn engine.

- Hydrogen engine can achieve similar efficiency under the various limitations to the methane burning engine when pre-chamber ignition system is employed.

- Hydrogen stoichiometric operation with EGR can achieve a relatively high efficiency (approximately 39%) only with a single stage turbocharger.

Contents

Abbreviations

0-D	Zero-dimensional
1-D	One-dimensional
bTDC	before top dead centre
CHP	Combined heat and power
CO_2	Carbon dioxide
deg	degrees crank angle
EGR	Exhaust gas recirculation
H_2	Hydrogen
NO_x	Nitrogen oxides
ICE	Internal combustion engine
KI-index	Knock intensity index
MAPO	Maximum amplitude of pressure oscillation
OC	Open-chamber
PC	Pre-chamber

1 Introduction

1.1 Background information and current situation

The European and global energy system faces an enormous challenge as it should satisfy the ever-rising energy demand, while mitigating CO_2-emissions [1]. While it is yet uncertain which of the available technologies (battery electric vehicles, fuel cells or internal combustion engines) will become the most dominant in the future, it seems that each transportation sector would require a mix of these technologies for an effective and holistic de-carbonization [2, 3]. In addition, certain sectors which require high energy density carriers and converters such as the long-haul shipping and aviation are expected to have a growing impact on the overall CO_2 emission in the near future [4, 1], due to globalization and further development of emerging economies.

Until batteries reach a significantly high density, fast charging times and the supporting infrastructure develops sufficiently, alternative fuels or e-fuels produced by renewable electricity can serve as the near term solution. These can be easily integrated in the existing gas grid and used in internal combustion engines. One of the most prominent such energy carrier which is also deemed as the fuel of the future is hydrogen. Hydrogen can be produced through a number of ways either from natural gas, biogas or water electrolysis [5]. Production and storage of hydrogen is gaining a lot of attention due to the potential of mitigating the fluctuating production of renewable electricity, predominantly through solar and wind. The cost of green hydrogen production is expected to further decline in the following years [6] making it comparable to conventional fuels according to some forecasts (especially if a carbon-tax is imposed).

Hydrogen can be used in a number of ways, either directly for power generation (in a fuel-cell or an internal combustion engine) or converted into an easier-to-handle gas with the so called "power-to-gas" applications. The use of hydrogen in fuel cells is the main alternative to the battery-based transportation systems offering higher energy density and fast fueling times. Combustion of hydrogen in internal combustion engines has been successfully demonstrated [7] and is particularly attractive for heavy duty applications owing to the high energy density of combustion-based energy converters. While nitrogen oxides (NO_x) emissions are produced in hydrogen internal combustion engines, they can be mitigated with exhaust gas after-treatment. In addition, since the efficiency of an internal combustion engine increases with its size [8], an internal combustion engine is desirable for high power density applications. In comparison to a fuel cell, an internal combustion engine is resistant to hydrogen impurities and can operate even with a combination of fuels [9], making it very robust and flexible.

Existing combustion-based technologies for medium size heavy duty engines are mostly concentrating on lean-burn concepts where natural gas is the primary fuel and hydrogen is used as an admixture [10]. Hydrogen addition allows for a reduction of cardon-related emissions, extension of the lean misfire limit and higher combustion stability [11]. The favorable hydrogen combustion characteristics are mainly linked with its high laminar flame speed, the wide flammability limits, the reduced ignition energy and small quenching distance [12, 13].

Due to the attractiveness of hydrogen as a clean combustion fuel, H_2-ICE have been investigated by numerous researchers [14, 15, 16]. Hydrogen's wide flammability limit enables H_2-ICEs stable operation with extremely lean mixtures [17, 18] or a combination of a lean air-fuel mixture and EGR [19, 20, 21]. This allows reduction of engine-out NO_x emissions due to the lower combustion temperature under high dilution conditions.

An alternative operation strategy to the employment of a lean air-fuel mixture constitutes the operation with stoichiometric mixture and EGR along with the use of a three way catalyst for after-treatment of NO_x. While this combustion technology has been extensively investigated for heavy duty natural gas (with or without H2 enrichment) internal combustion engines [22, 23, 24] and even H_2-fueled small engines [25], it remains relatively unexplored for H_2-fueled medium size heavy-duty IC engines.

Nonetheless, very promising experimental results from the application of this concept in a H_2-fueled stationary engine without aftertreatment have been demonstrated very recently [26]. The results showed that extreme levels of EGR can suppress NO_x emission and the occurrence of abnormal combustion with little to no impact on the overall engine efficiency, while simultaneously achieving very high power output. This calls for further investigation of this combustion technology for identification of potential gains and limitations.

1.2 Purpose of the project

The project aims at comparing two different combustion technologies (lean burn against stoichiometric operation with exhaust gas recirculation) on a heavy duty hydrogen combustion engine by means of one-dimensional numerical simulations. The performance and efficiency of the H_2-ICE on steady-state/full load operation and under different limitations (knocking, maximum cylinder pressure, turbine inlet temperature among others) is sought.

1.3 Objectives

The overall objectives of the research project are: (i) to identify the achievable limits in thermodynamic efficiency, power-density (preferably with single-stage turbo-charging), NO_x-emissions, for a heavy-duty H_2-engine, (ii) to compare the lean burn operation against stoichiometric operation with EGR with both methane and hydrogen as fuels including open and pre-chamber configurations and (iii) to develop an easy to use simulation tool for fast and accurate evaluation of various design and operating parameters on the hydrogen engine performance and emissions. For this purpose, an existing phenomenological PC combustion model (Diss. K. Bardis, LAV, ETH) is extended with additional sub-models for knocking and NO_x emissions. Appropriate modifications are made to account for the specifics of hydrogen combustion. Finally, the phenomenological combustion model is integrated into a commercially available simulation software (GT-Power) which provides the initial conditions for the power cycle.

2 Procedures and methodology

2.1 Phenomenological Combustion Model

The basis of the combustion model for the PC engine has been already described in detail in earlier work of the authors [27]. It consists of a two-zone thermodynamic model (in each control volume) and detailed phenomenological models for both the pre- and main chamber heat release rates. Various sub-models for the jet penetration, turbulence, ignition and flame wall interaction are included to account for the most dominant phenomena inside such an engine as well as their interaction. A schematic overview of the model is given in Figure 1.

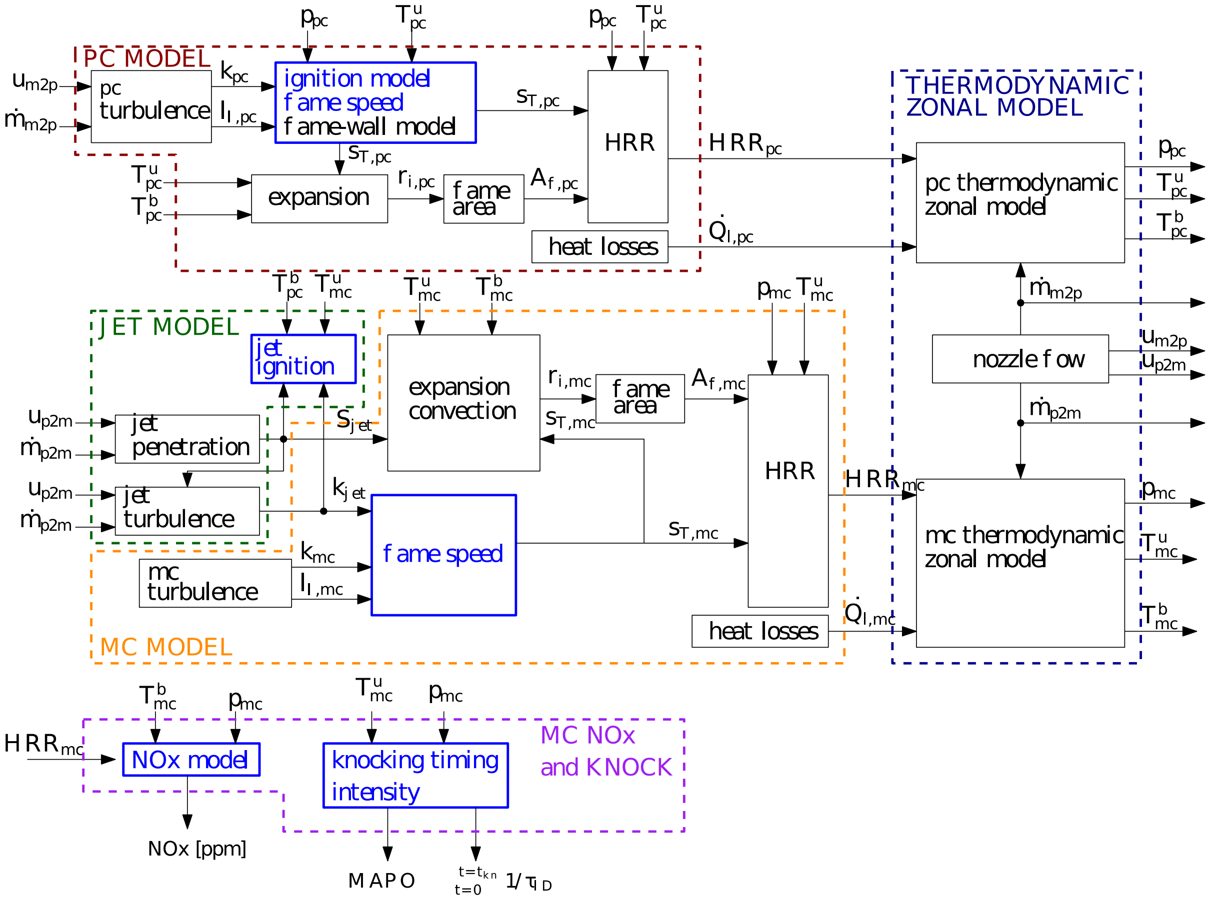

Figure 1. Quasi-dimensional model schematic overview.

Apart from the obvious adaptation of the thermodynamic properties and the chemical kinetics (for the flame speed calculation and the ignition delay) the ignition model for the pre- and main-chamber are adapted to account for the effect of hydrogen. All sub-models which are influenced by the hydrogen chemistry (apart from obvious changes of the properties) are shown with blue in Figure 1. The quasi-dimensional model is extended with two additional sub-models for the NO_x formation and knocking intensity (shown within the purple box of Figure 1), which are described in detail below. In addition, the quasi-dimensional model is coupled to the well-known 1-D simulation software GT-POWER such that the gas dynamics and the interaction with the turbocharger can be accounted for.

In addition to the PC simulations, conventional OC simulations were conducted. This is motivated by the fact that the flame speed of hydrogen is higher than this of methane-air mixture and the minimum ignition energy of hydrogen is significantly lower than this of methane-air mixtures, which both increase the combustion stability and burning rates. The model for the conventional spark-ignition engine is based on the classical assumption of spherical flame speed propagation inside the combustion chamber [8]. A simple Damköhler correlation was employed as a turbulent flame speed closure. In the present section, the term main-chamber refers by definition to the combustion chamber of the spark-ignited engine.

2.2 NO_x and Knock Models Development

The thermodynamic model provides the pressure, unburned and burned temperature traces as well as the volume occupied by each zone for both the pre and main-chamber. Based on the unburned temperature and the main chamber pressure the knock propensity can be estimated. The knock model consists of two components: a knock integral through which the knock initiation is determined and a knock intensity index (KI-index). Equation 1 provides the knock criterion based on the integral of the inverse of the ignition delay. The value of the knock integral is determined for a burned mass fraction of 80%, since knocking is unlikely to occur beyond this mass fraction as the flame is already within the cold wall boundary layer [28].

$$\int_{t=t_{ST}}^{t=t_{x_b=80\%}} \frac{dt}{\tau(p, T_u, \lambda, x_{EGR})} \geq 1 \qquad Eq. (1)$$

The ignition delay is tabulated from zero-dimensional (0-D) homogeneous reactor calculations, which are carried out with the Cantera plug-in for Matlab/Simulink [29]. Figure 2a and 2b show an example of such a calculation for the evolution of temperature and heat release rate in a 0-D reactor. The ignition delay time is defined as the time instant that 5% of the maximum of the heat release rate is reached.

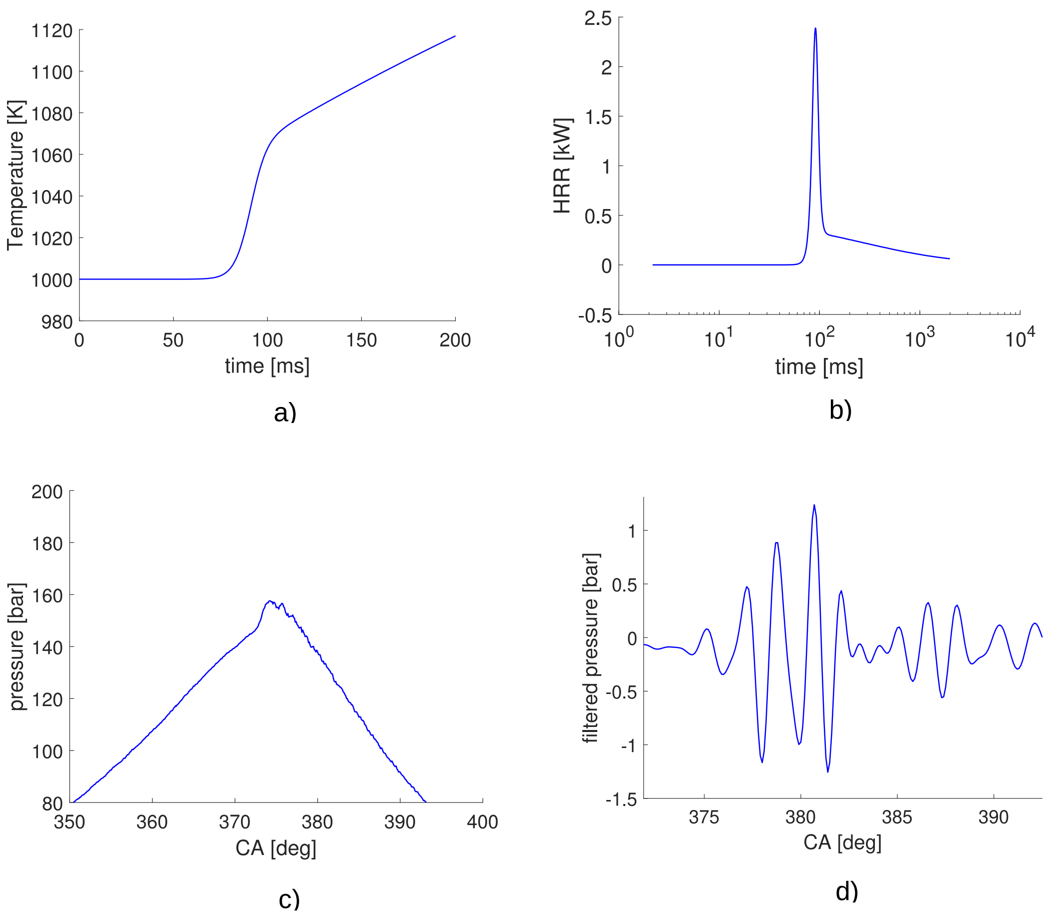

Figure 2. Variation of the temperature (a) and the heat release rate (b) for a 0-D reactor at initial condition: (p,T,λ,EGR) = (150 bar, 1000 K, 2.0, 0.0). Cylinder pressure at a point of knock occurrence (c) and the corresponding filtered pressure signal (d) [1].

While the knock integral criterion is necessary to determine whether knocking actually occurs, it does not indicate the knocking intensity and, therefore, if knocking is detrimental for the engine operation. The indicator of knocking intensity is the maximum amplitude of pressure oscillations (MAPO). This value is the maximum of the filtered pressure trace within the frequency range of knock occurrence. Figure 2c shows an example of a pressure trace along with the filtered pressure signal in Figure 2d for the G946 LMB engine. In this case MAPO is approximately 1.2 bar which corresponds to mild knock.

In the developed model, it is assumed that knocking is triggered by temperature inhomogeneities within the cylinder (hot spots), which auto-ignite and generate detonation waves [30]. It should be mentioned that this is one mode of knock initiation, as hot-surface ignition, for instance, can also lead to knocking. This aspect may be crucial for hydrogen, for which the minimum ignition energy is low, and should be accounted for in a future study. While MAPO cannot be directly computed from a low order simulation, it was observed that it correlates almost linearly with the knock intensity index (KI-index) [31, 32]. The KI-index is determined from the following expression

[1] Figures order: counter clockwise.

$$KI = 2\,\xi^{-2} p_{mc} \qquad Eq.(2)$$

according to [30]. The calculation is based on the resonance parameter ξ of the hot spot and the pressure p_{mc} inside the engine combustion chamber. The resonance parameter describes the coupling between the acoustic wave and the propagation of the reaction front; it is given as the ratio of the acoustic to the autoignition propagation velocity

$$\xi = \frac{\sqrt{\gamma RT}}{\frac{\partial r}{\partial T}\frac{\partial T}{\partial \tau_{ID}}} \qquad Eq.(3)$$

The temperature gradient of the ignition delay can be easily tabulated from the zero-dimensional ignition delay calculation described earlier. The inverse of the mean temperature gradient was taken 0.5 mm/K which is a typical value for engine-relevant conditions [32].

Nitrogen-oxides emissions consist of nitric oxide (NO) and nitrogen dioxide (NO_2). The main part of the NO_x emissions is made of the nitric oxide. To describe the formation of NO the reduced Zeldovich mechanism is applied [8]

$$O + N_2 \rightarrow NO + N$$

$$N + O_2 \rightarrow NO + O$$

$$N + OH \rightarrow NO + H$$

where [N] is assumed to be in steady-state and that the concentration of all species apart from NO are in equilibrium. Provided this assumption, the differential equation describing the evolution of nitric oxide can be written as [8]

$$\frac{dNO}{dt} = C_{ZM} 2R_1 \frac{1 - \left(\frac{[NO]}{[NO]_e}\right)^2}{1 + \left(\frac{[NO]}{[NO]_e}\right)\frac{R_1}{R_2 + R_3}} \qquad Eq.(4)$$

with

$$R_1 = k_1\,[O]_e[N_2]_e$$

$$R_2 = k_2[N]_e[O_2]_e$$

$$R_3 = k_3[N]_e[OH_2]_e$$

The reaction rate constants (k_1, k_2, k_3) are set the to the standard values given by [8]. It should be noted that the calculation of the NO_x formation remains virtually the same for hydrogen, with the only difference being that the equilibrium constants contain different species.

2.3 Hydrogen Combustion Model

The base PC combustion model was modified to account for the specifics of the hydrogen combustion. One basic adaptation is the use of the laminar flame speed for hydrogen-air mixtures. The planar laminar flame speed is determined with one-dimensional steady state laminar flame speed calculation using the Cantera plug-in for Matlab/Simulink [29] employing a reduced hydrogen combustion mechanism [33].

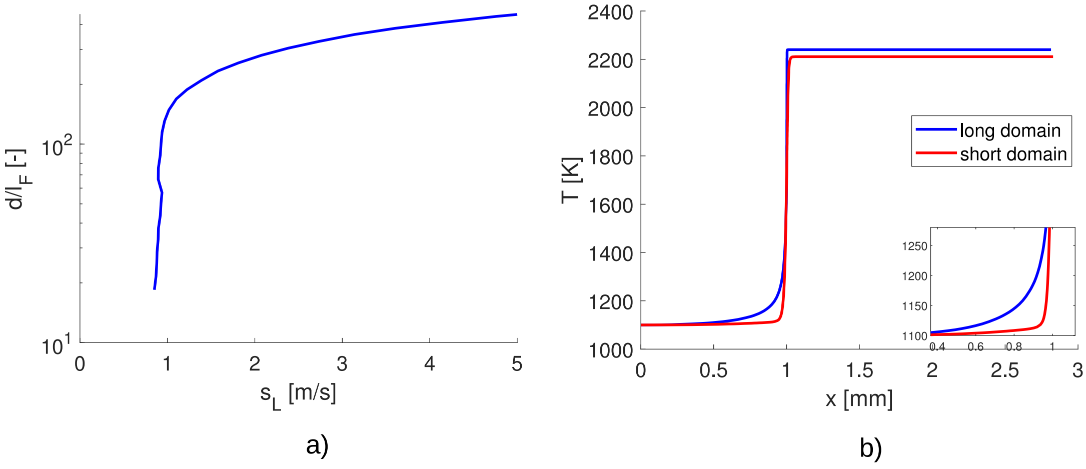

Figure 3. a) Variation of the flame speed with the domain size (normalised with the flame thickness). b) Temperature variation across the domain for a long (blue) and short (red) domain: both figures refer to a lean hydrogen-air mixture with: lambda = 2.20, pressure = 150 bar, temperature = 1100 K.

Special care is taken to consistently determine the laminar flame speed under (or near) auto-igniting conditions [34, 35]; this is particularly important for hydrogen-air mixtures as the high reactivity increases the propensity of auto-ignition. Figure 3a shows the variation of the laminar flame speed as derived from one-dimensional planar flame over the domain size (normalized with the flame thickness) for a mixture of hydrogen and air with lambda = 2.2, p = 150 bar and T_u = 1100 K. It can be seen that for reducing domain size the laminar flame speed asymptotically approaches its actual value.

However, for very long domain size, autoignition is triggered resulting in an increase of pressure and temperature and modification of the actual conditions of flame propagation. This creates an apparent laminar flame speed higher than the actual, since the reference conditions are no longer the ones at the boundary but the ones after auto-ignition. Figure 3b depicts the temperature variation inside the domain for two different domain sizes. For the long domain size, auto-ignition was triggered before the heat diffusion results in significant increase of the unburned side temperature.

To guarantee consistent computation of the laminar flame speed, the laminar flame speed is calculated using the one-dimensional premixed flame simulation for various domain size. The final flame speed is determined such that the following convergent criterion is met: the difference in the computed flame speed of two consecutive domain sizes is below 1%. This occurs when the domain size is in the range of 10 to 50 multiples of the flame thickness. As can be seen in Figure 3a, the flame speed has already converged in this range.

The mechanisms of turbulent jet ignition are also dependent on the fuel employed [36]. Figures 4a and 4b depict the combined reaction-diffusion for various mixing rates (expressed with the maximum of the scalar dissipation rate) during the turbulent jet ignition in the mixture fraction and progress variable space for a hydrogen and methane mixture, respectively. The reaction source term is obtained from the solution of the 1-D flamelet equation and represents the inverse of the ignition delay time. As it can be seen a mixture of hydrogen-air is more resistant to flame quenching in comparison to a methane-air mixture [37], which is manifested by the higher quenching mixing rate. In addition, the hydrogen-air mixture source term is at least double of that of the methane, resulting in smaller ignition delay time for hydrogen. This results in faster and more stable ignition (reduced quenching propensity) for hydrogen-air mixtures.

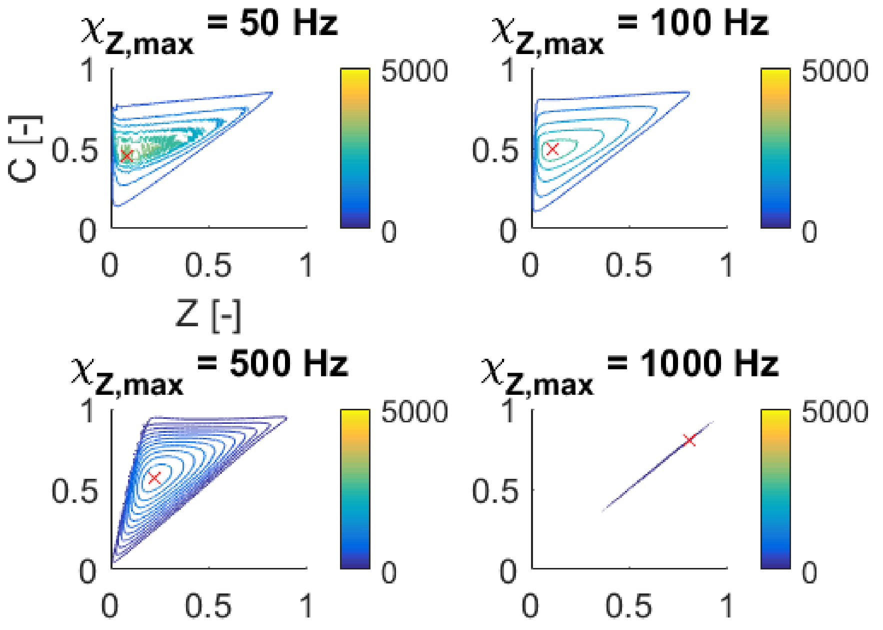

a)

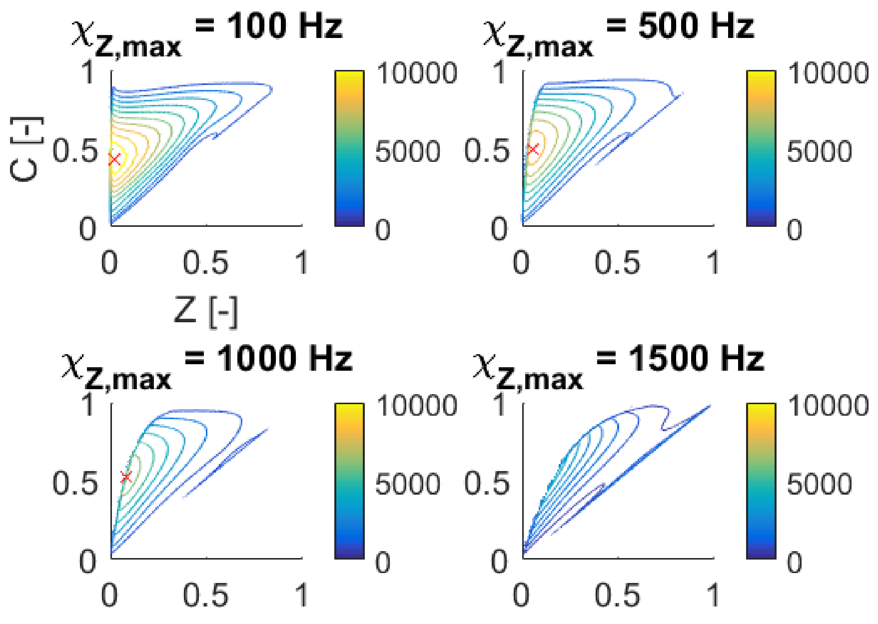

b)

Figure 4. Contour plot of the combined reaction-diffusion term in the 1-D flamelet equation as a function of the mixture fraction Z and progress variable C for four levels of the maximum scalar dissipation rate $\chi_{Z,max}$ (expressing the mixing intensity) for (a) a methane-air (top 4 figures) and (b) a hydrogen-air mixture (bottom 4 figures) at atmospheric conditions.

2.4 Numerical Implementation

The PC combustion model developed in [27] and extended in the present article provides the evolution of the thermodynamic variables during the closed valve engine cycle. When the valves are open, enthalpy and mass is exchanged with the intake and the exhaust manifold. This affects the pressure and temperature at the beginning of the closed valve cycle, the turbulence and the mixture composition inside the cylinder.

GT Power offers a well-established framework for modelling the various components in internal combustion engines, such as the piping, turbocharger, engine cylinder among others. It allows for accurately description of the gas dynamics that occur in the pipes and manifolds, which are numerically challenging to capture. It is, therefore, advantageous to use this commercial software in order to obtain the initial conditions for the power cycle. In order to achieve this objective, the complete combustion code is converted from the original Matlab script into C code and integrated in the engine cylinder user-code module of GT-Power. During the code conversion, certain modelling components are adjusted due to the special requirements of a low-level language. An advantage of the conversion is the acceleration of the power cycle simulation by a factor of five, from approximately 2 min to 25 sec. This can significantly accelerate the simulation of multiple operating points and is crucial for the simulation of the multi-cylinder engine.

During the gas-exchange no data are passed between the user-code and the GT Power. At the intake valve closure, the in-cylinder conditions are transferred from the GT-Power into the user-code. The user-code becomes active after this time instant and is used to compute the in-cylinder conditions such as pressure, temperature and mixture composition. Certain variables, such as the pressure, are passed into the GT-Power simulation, since they influence the instantaneous compression work to the piston and ultimately the full engine cycle.

3 Results and discussion

3.1 Model Validation

The methane combustion model has been extensively validated in an earlier work of the authors [27, 38] for the two Liebher lean-burn gas engines and under different conditions. This ensures accurate description of the thermodynamic variables, which are inputs to the knock and emissions models.

No experimental data were available for a pure hydrogen combustion engine. The hydrogen combustion model accuracy is, therefore, predominantly linked with the accuracy of the chemical mechanism that are employed for the computation of the laminar flame speed and the turbulent flame speed closure accuracy when hydrogen is employed as fuel. Hydrogen combustion chemistry is less complex when compared to methane combustion and, therefore, the uncertainty introduced by the chemical kinetics in the laminar flame speed computations is limited. In addition, while hydrogen has a significantly higher flame speed in comparison to methane, the air-to-fuel ratio is significantly higher. This results in similar reactivity and effective dilution conditions.

Table 1. Liebherr G96 engine specifications.

Engine Configuration	G-96
Displacement Volume	2.43 L/Cyl
Stroke	170 mm
Bore	135 mm
Number of Valves	4
Rated Power	50 kW/Cyl (50Hz)
Rated Speed	1500 rpm (50Hz) / 1800 rpm (60Hz)
lambda	1.735
ST	13 deg bTDC

Before proceeding with the evaluation of the different combustion concepts, the GT-Power model with the integrated phenomenological power-cycle module is compared against a GT-Power model provided by Liebherr with adjusted Wiebe-function parameters and NO_x model constants to exactly match the experimental results of the given engine. Therefore, this comparison should be a direct indicator of the model performance against the experimental data, and, for this reason, to avoid any confusion it will be referred as experiment in the present section. Table 1 provides the specifications of the lean-burn natural gas engine along with the operating conditions. The basic performance and emission outputs for the two simulations are given in Table 2.

Table 2. Reference point performance and emission parameters.

parameters	experiment	simulation	difference in %
brake power [kW]	984.8	999.8	1.52
imep [bar]	17.32	17.57	1.44
engine speed [RPM]	1500	1500	0
brake efficiency [%]	42.23	40.70	-3.62
air flow rate [kg/h]	5008	5276	5.35
compressor pressure ratio [bar]	3.538	3.799	7.37
turbine power [kW]	250.25	283.43	13.25
turbine inlet temperature [K]	877.63	873.94	0.42
peak pressure [bar]	113.52	114.50	0.86
crank angle of maximum pressure [deg]	17.43	19.25	10.44
NO_x emissions [ppm]	62.72	92.46	47.41

The model performs fairly well. However, small differences are evident as is the case for example for the brake efficiency which is underestimated by 3.62% by the predictive combustion model. Due to the difference in the efficiency, the compressor has to provide an increased boost pressure such that the same engine power output is achieved (about 7.37% increased pressure ratio). The exhaust gas temperature is very closely matched by the model with less than 2°C difference.

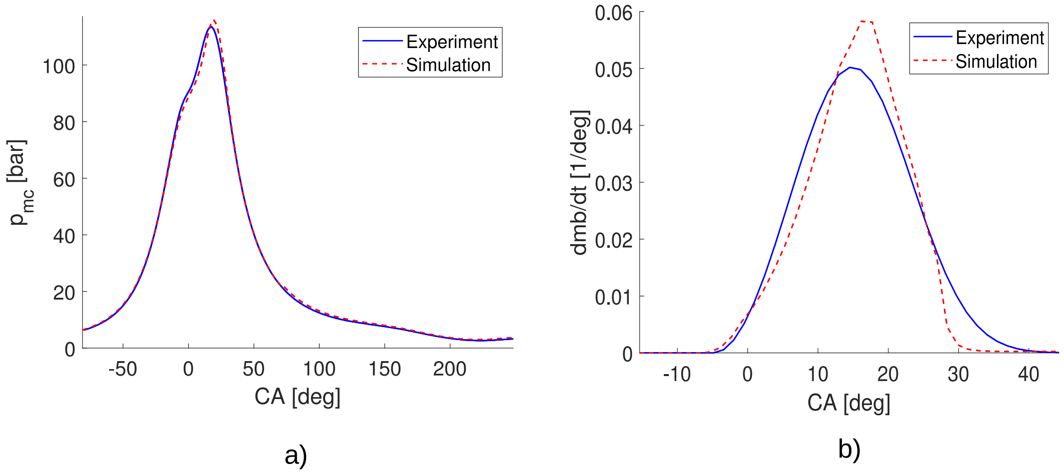

Figure 5. Comparison of the main chamber (a) cylinder pressure (left) and (b) heat release rate (right) from the experiment (blue solid line) against the simulation using the predictive combustion model (red dashed line).

Looking into more detail the in-cylinder parameters, the model is able to provide a very good prediction of the maximum pressure, which differs by only 0.86% from the experiment. The crank angle of the maximum pressure is about 1 degrees crank angle different between the simulation and the experiment. From the comparison of the complete pressure trace and heat release rate given in Figure 5a and 5b, respectively, it can be seen that the predictive model matches closely the experiment. Nonetheless, it is apparent that the burning rate of the predictive combustion model is slightly lower during the early phase than the one of the experiment. This results in a higher maximum pressure for the same spark timing such that the same power output is achieved.

The NO_x differ by about 47% between the simulation and the experiment. While this difference is rather high, it arguably challenging to obtain accurate NO_x prediction with a low order model. Additionally, small differences in the combustion burning rate (as is the case here) may result in significant error in NO_x emissions prediction. Despite the differences presented, the model performance is reasonable given that it was calibrated for a different engine (G-946), prechamber (M-18) and operating conditions. The model contains certain tuning parameters which were kept unchanged from the original calibration. These parameters can be very easily adjusted to achieve a perfect fit with the LMB simulation, especially when the match with a single point is sought. The uncertainty of the extrapolation is in any case present and the relative differences are not significantly affected by the initial calibration.

3.2 Comparison of Lean vs. λ=1+EGR

In this section the results from the numerical simulations with various configurations are presented. All the simulations for methane are carried out in the lean limit which yields the lowest NO_x and the highest engine efficiency due to the minimization of the heat losses. On the contrary, for hydrogen a reduce lambda in comparison to the lean limit is employed which reduces the pumping losses due to the less amount of air that need to inducted.

3.2.1 Open-chamber combustion

Figure 6 depicts the predicted brake efficiency, nitrogen oxides emissions, the maximum amplitude of pressure oscillation, the pressure ratio over the compressor, the maximum cylinder pressure and the turbine inlet temperature for a variation of the spark timing for methane-lean (solid blue) and methane-stoichiometric operation with EGR (dashed blue). Along with the simulation results, the different engine limits are shown. These are the following: 1) the NO_x limit at 100 mg/m3 and 500 mg/m3 (depending on the current legislations) 2) the knock limit at MAPO = 2 bar for mild and at 3bar for hard knock 3) the boost pressure limit at 4.5 bar, above which a two stage turbocharger is needed to achieve the desired compression power, 4) the maximum pressure limit of the G-9620 engine at p = 150 bar that stems from mechanical limitations of the engine and the 5) engine outlet temperature limit that is based on the thermal strength of the turbine blades. It should be mentioned that the above limits refer to the given engine; for instance, it is not uncommon that the allowed maximum pressure is higher than 150 bar. In addition to the above, the reference point is shown with purple star and the best point for each operating concept with blue star, blue circle, green star and green circle for the lean methane, λ=1+EGR methane, lean hydrogen and λ=1+EGR hydrogen operation, respectively. In both operating models, the brake power of the engine is 1 MW_{el} and the engine speed 1500 RPM. The lambda value is set to 1.735 for the lean operation and the EGR-rate to 22.5 % for the stoichiometric operation with EGR. These values are both near the dilution limits, since it was observed that a richer mixture results in inferior performance in terms of engine efficiency and NO_x emissions.

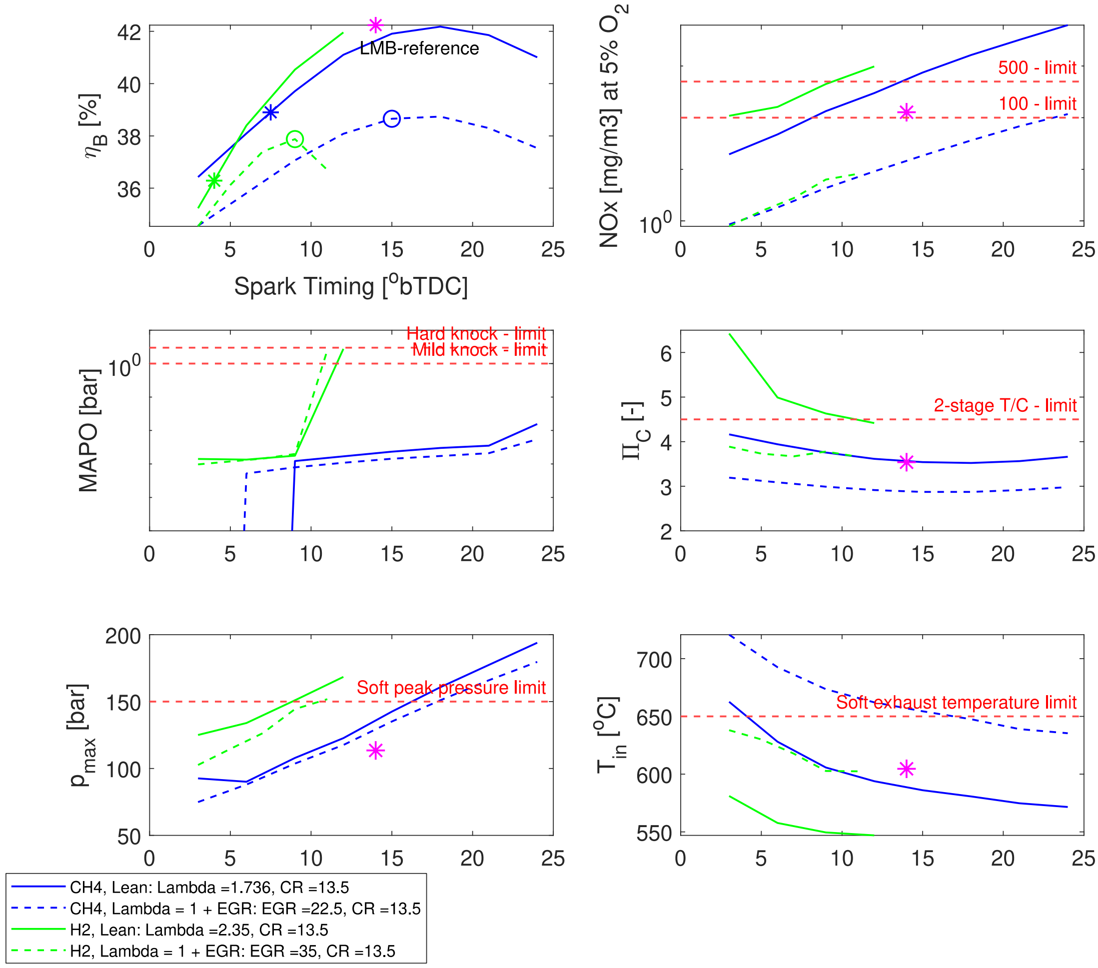

Figure 6. Open-chamber operation: Variation of the brake efficiency, NO_x, MAPO, compressor pressure ratio (Π_c), maximum pressure and intake temperature with the spark timing for lean (solid line) and stoichiometric operation with EGR (dashed line) with methane (blue) and hydrogen (green) as fuel. Shown with dashed red line are the various limits of the engine.

The brake efficiency maximum is 42.2% and 38.73% for the methane lean and lambda = 1 + EGR, respectively, which corresponds to a spark timing of 18 and 15 deg bTDC, respectively. This difference is due to the higher heat losses and the reduction of the specific heat ratio (c_p/c_v) due to the water vapour content, which influences the theoretically maximum efficiency of the engine. This is a known negative aspect of the lambda = 1 + EGR operation which has been observed in previous experimental studies [24]. The lower efficiency results in a high temperature before the turbine as the exhaust enthalpy is higher.

While the efficiency of lean operation is high, the best-efficiency point lies well above the legislated emission limits. The efficiency of lean operation within the allowed NO_x (assuming NO_x legislated emissions at 100 mg/m3) is approximately 39.0% and corresponds to a spark timing of 8 deg bTDC. This value is slightly higher than the 38.73% of the lambda = 1 + EGR operation. The maximum efficiency of the lambda = 1 + EGR operation is primarily limited by the exhaust gas temperature and the peak pressure limit. It can be observed that for ST = 15 deg bTDC, the exhaust temperature is slightly, by few degrees Celsius, above the assumed limit.

In terms of maximum pressure and knocking intensity, the lambda = 1 + EGR operation is very similar to the lean burn operation. An evident difference between the two concepts relates to the significantly reduced boost pressure requirement for the lambda = 1 + EGR operation to deliver the same power output. This due to the reduced amount of air delivery for the stoichiometric engine in comparison to the lean-burn engine. Additionally, the NO_x emissions of the lambda = 1 + EGR stoichiometric operation are significantly lower than for lean operation. It should be mentioned that the NO_x emissions for lambda = 1 + EGR operation refer to the ones after the catalyst, assuming a conversion efficiency of 98%, which is common under steady state engine operation.

For the hydrogen operation, the lambda value and EGR rate were adjusted to achieve similar effective dilution and reactivity conditions as with the methane. The hydrogen engine produces 1 MW_{el} brake power at an engine speed of 1500 RPM. After experimentation with different value for the lambda and EGR-rate the following values were selected: lambda = 2.35 and EGR = 35. The lambda value is reduced in comparison to the hydrogen lean limit but results in a reduction of air delivery requirement and, consequently, the pumping losses. This allows for a higher engine efficiency to be achieved with reasonable turbocharging power.

Hydrogen lean operation results in significantly lower efficiency (approximately 36.5%) compared to methane lean operation due to the increased NO_x emissions, which necessitate for a drastically retarded spark timing in comparison to the optimal. Another reason for the reduced efficiency is the higher pumping losses (approximately 1 bar for hydrogen, compared to 0.5 bar for methane-lean operation) due to the increased requirement for compression of the trapped mixture. In addition to the NO_x limitation, the efficiency of hydrogen-lean operation is limited by the knocking and the maximum pressure limit. Due to the higher reactivity of the hydrogen mixtures, auto-ignition is more likely to occur in comparison to methane operation. The required amount of boost pressure essentially makes the hydrogen-lean burn operation only possible with a two-stage turbocharger, resulting in increased cost and complexity.

On the contrary, lambda = 1+EGR hydrogen operation drastically mitigates the required boost pressure requirement that severely limits hydrogen lean operation. Thanks to the high conversion efficiency of the exhaust gas after-treatment under steady conditions, NO_x emission are well below the legislated limits. A brake efficiency of 37.8% is achieved with all limitations being respected. This is higher than the one of the lean operation and demonstrates that different operating concepts might be more suitable with different fuels.

3.2.2 Pre-chamber combustion

For the prechamber operation the same engine operation and dilution conditions as for the open-chamber were selected. Since the present prechamber is unscavenged, the lean limit does not significantly differ from the one with OC.

The pre-chamber methane operation shows similar trends to the open-chamber engine operation. While combustion proceeds rapidly after the turbulent jet ignition, the initiation of combustion in the main chamber is dictated by the reactive jet exit timing, which delays due to the prechamber combustion and the mixing-induced extinction. These two conflicting trends result in a best efficiency spark timing similar to the one observed in the OC operation. The maximum efficiency is slightly higher compared to the OC engine thanks to the faster consumption of the main chamber mixture by the multiple jets and the turbulence generation in the vicinity of the flame front. In addition, the efficiency is seen to be less sensitive to the employed spark timing in comparison to OC operation. This is likely due to the fast consumption of the main chamber mixture by the turbulent jets and the dominant effect of the generated turbulence; in other words, the thermochemical conditions has less of an impact.

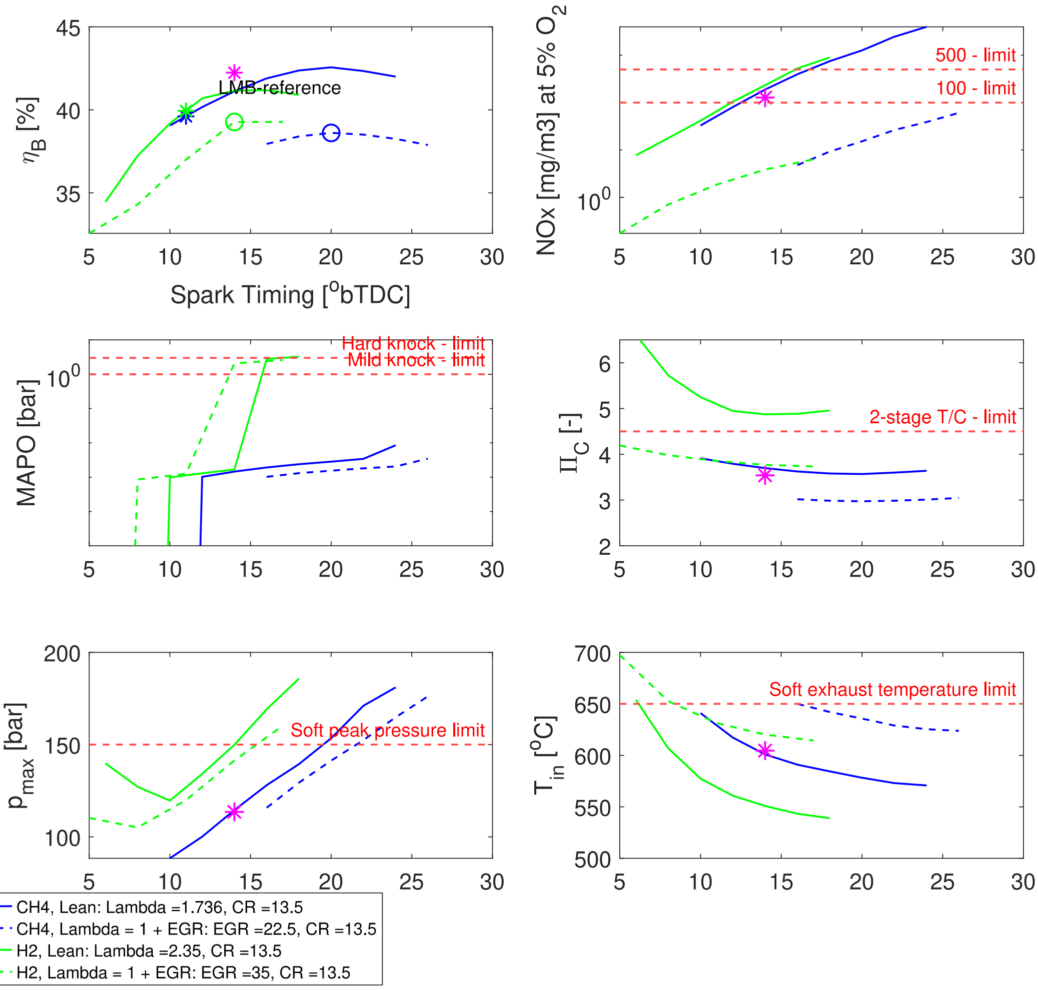

Figure 7. Pre-chamber operation: Variation of the brake efficiency, NOx, MAPO, compressor pressure ratio (Π_c), maximum pressure and intake temperature with the spark timing for lean (solid line) and stoichiometric operation with EGR (dashed line) with methane (blue) and hydrogen (green) as fuel. Shown with dashed red line are the various limits of the engine.

The variation of the brake efficiency shows the classical inverse U-shaped profile and presents a maximum at about 42.5%, which corresponds to a spark timing of 20 deg bTDC. However, due to the high combustion temperature, the NO_x are higher than 500 mg/m3 at the optimal efficiency point. A different operating condition with acceptable NO_x (for a strict emission limit) corresponds to spark timing 11 deg bTDC and an efficiency of approximately 40.1%. All other variables are well below the various limits for this point. It can be concluded further, that the PC operation offers an advantage in comparison to the conventional spark-ignited engine in terms of increased efficiency, under NO_x limited operation, by approximately 1%.

Comparing the lambda = 1 + EGR against the lean burn methane engine, it can be seen that the latter achieves a lower efficiency of about 38.5% in the best point. All variables are well below the set limits in this operating condition. The difference is, therefore, greater in comparison to the spark-ignited engine and justifies the employment of lean operation when the engine is equipped with a prechamber. However, when hydrogen is employed as fuel this stoichiometric operation with EGR is clearly superior.

For the hydrogen lean burn concept with pre-chamber, the best efficiency point is very similar to the methane lean operation. However, the air delivery requirement necessitates for increased boost pressure and potentially two stage turbocharger. Similar to the trends observed with the OC, the prechamber allows for increased efficiency under the NO_x limitation. In the case of hydrogen, the difference between open and pre-chamber is very pronounced and the efficiency gain is approximately 3.6% .

Employment of stoichiometric mixture with EGR for a hydrogen engine equipped with prechamber yields significant reduction on the required boost pressure. The efficiency is only minor affected by the switch from lean to stoichiometric operation. This is mainly attributed to the significant reduction of the pumping losses, which partly compensates the decreased thermodynamic efficiency due to the lower specific heat ratio (c_p/c_v) by the water vapour content. With exhaust gas after-treatment the engine is virtually NO_x free. It should be mentioned that the mild knocking observed in the near optimum spark timing might require a slightly retarded advance angle with a small penalty in efficiency.

4 Conclusions

In this study the lean engine concept was compared against stoichiometric operation with high levels of EGR for a heavy duty engine including two different configurations: open and pre-chamber. Base-line simulations were carried out with methane as fuel in order to verify previous experimental results and contrast them to the newly obtained hydrogen combustion simulations. The most important conclusions of the present study are the following:

- In terms of modelling and combustion phenomenology:
  - The one-dimensional laminar flame speed calculations under near autoignition conditions have to be carried such that the autoignition time scale is smaller compared to the flame time-scale. This is achieved by employing a domain size which is small enough such that autoignition is suppressed and guarantees consistent flame speed calculation.
  - Hydrogen presents both higher resistance to flame extinction (expressed with a higher scalar dissipation rate for extinction) and higher reactivity. These two combined result in smaller ignition delay time after extinction of the flame during turbulent jet ignition as well lower quenching propensity.
- In terms of the engine operation:
  - The employment of unscavenged prechamber results in small increase of the maximum efficiency, but notable gain in the NO_x limited engine efficiency. This is particularly pronounced for the hydrogen lean operation.
  - Hydrogen operation requires for optimal thermodynamic efficiency later spark timings due to its higher flame speed and, therefore, shorter combustion duration.
  - Hydrogen lean operation with prechamber can achieve similar efficiency to the methane lean operation. This is a result of the increased pumping losses which compensate the increase of efficiency by the faster combustion when hydrogen is employed as fuel.
  - Hydrogen lean operation is only possible when a two-stage turbocharger is employed.
  - The employment of stoichiometric operation with EGR results in significant reduction of the required boost pressure, which in conjunction with the reduction of NO_x emissions with appropriate exhaust gas aftertreatment allows for relatively high engine efficiency.

5 Outlook and next steps

This research project constitutes an important first step towards the simulation based evaluation of different combustion concepts for hydrogen heavy duty engines which are expected to play a major role in the future energy system. The model developed can be easily employed for the thermodynamic optimisation of such engines and provide valuable insights for the design of future experiments in a cost-effective manner. Thanks to the development and inclusion of additional sub-models for knocking intensity and NO_x emissions, as well as the development of hydrogen specific combustion models, the effort required to obtain practical insights is minimal.

In view of the absence of experimental data for a hydrogen fuelled engine, it is necessary to validate or revise some key assumptions for the engine operation with hydrogen referring to the potentially increased wall heat losses, the not quantitatively known self-ignition trends on hot surfaces of the combustion chamber and the flame speed of H_2-air mixtures at engine-relevant temperatures and pressures. Additionally, it is necessary to explore benefits of direct in-cylinder fuel injection and the additional optimization potential of the compression ratio for the case of hydrogen.

Therefore, we recommend to set-up experimental projects to eliminate such uncertainties and clarify additional optimization measures for H_2-fuelled internal combustion engines. One such fundamental research project is already starting at EMPA in cooperation with Stuttgart University in the CORNET-framework (co-funded by BFE and FVV), while another one could possibly be carried out on the application side using a multi-cylinder engine. Including related experience, if available, at Swiss industrial companies would be an additional meaningful next step.

6 National and international cooperation

The GT-Power model for the baseline methane engine was provided by Liebherr. The project partners wish to express their gratitude to the colleagues from Liebherr for their support.

7 Communication

Hydrogen Combustion Engines Workshop, 19th of August 2021, online meeting via Zoom with 18 participants from Swiss Academia and Industry

The meeting minutes can be found in the Appendix.

8 Publications

Bardis K, Boulouchos K, *Comparative simulation study of lean burn versus stoichiometric operation with EGR for a hydrogen heavy duty combustion engine*, in preparation for Journal of Engine Research (2021).

9 References

1. *BP Energy Outlook.* 2019 edition. London, United Kingdom, 2019.
2. Küng L, Bütler T, Georges G, and Boulouchos K. *Decarbonizing passenger cars using different powertrain technologies: Optimal fleet composition under evolving electricity supply.* Transportation Research Part C: Emerging Technologies, 95:785–801, 2018.
3. Wanitschke A and Hoffmann S. *Are battery electric vehicles the future? an uncertainty comparison with hydrogen and combustion engines.* Environmental Innovation and Societal Transitions, 35:509–523, 2020.
4. International Renewable Energy Agency. *Navigating to a renewable future: Solutions for decarbonising shipping.* IRENA, Abu Dhabi, September 2019.
5. Holladay JD, Jianli Hu, King DL, and Wang Y. *An overview of hydrogen production technologies.* Catalysis today, 139(4):244–260, 2009.
6. International Renewable Energy Agency. *Hydrogen: A renewable energy perspective.* IRENA, Abu Dhabi, 2019.
7. White CM, Steeper RR, and Lutz AE. *The hydrogen-fueled internal combustion engine: a technical review.* International journal of hydrogen energy, 31(10):1292–1305, 2006.
8. Heywood JB*. Internal combustion engine fundamentals.* Mcgraw-hill, 1988.
9. Verhelst S. *Recent progress in the use of hydrogen as a fuel for internal combustion engines. international journal of hydrogen energy*, 39(2):1071–1085, 2014.
10. Akansu SO, Dulger Z, Kahraman N, and Veziroglu TN*. Internal combustion engines fueled by natural gas-hydrogen mixtures.* International journal of hydrogen energy, 29(14):1527–1539, 2004.
11. Ma F, Wang Y, Liu H, Li Y, Wang J, and Zhao S. *Experimental study on thermal efficiency and emission characteristics of a lean burn hydrogen enriched natural gas engine.* International Journal of Hydrogen Energy, 32(18):5067–5075, 2007.
12. Kammermann T. *Optical Diagnostics of Ignition and Early Flame Kernel Formation in Premixed Hydrogen-Enriched Methane-Air Flames.* PhD thesis, ETH Zurich, 2019.
13. Gerke U, Steurs K, Rebecchi P, and Boulouchos K. *Derivation of burning velocities of premixed hydrogen/air flames at engine-relevant conditions using a single-cylinder compression machine with optical access.* International Journal of Hydrogen Energy, 35(6):2566–2577, 2010.
14. Karim GA. *Hydrogen as a spark ignition engine fuel.* International Journal of Hydrogen Energy, 28(5):569–577, 2003.
15. Verhelst S and Wallner T. *Hydrogen-fueled internal combustion engines.* Progress in energy and combustion science, 35(6):490–527, 2009.

16. Fayaz H, Saidur R, Razali N, Anuar FS, Saleman AR, and Islam MR. *An overview of hydrogen as a vehicle fuel.* Renewable and Sustainable Energy Reviews, 16(8):5511–5528, 2012.
17. Mohammadi A, Shioji M, Nakai Y, Ishikura W, and Tabo E. *Performance and combustion characteristics of a direct injection SI hydrogen engine.* International Journal of Hydrogen Energy, 32(2):296–304, 2007.
18. Francfort J and Karner D. *Hydrogen ICE vehicle testing activities.* Technical report, SAE Technical Paper, 2006.
19. Berckmüller M, Rottengruber H, Eder A, Brehm N, Elsässer G, Müller-Alander G, and Schwarz C. *Potentials of a charged SI-hydrogen engine.* Technical report, SAE Technical Paper, 2003.
20. Heffel JW. *NO_x emission reduction in a hydrogen fueled internal combustion engine at 3000 rpm using exhaust gas recirculation.* International Journal of Hydrogen Energy, 28 (11):1285–1292, 2003.
21. Heffel JW. *NO_x emission and performance data for a hydrogen fueled internal combustion engine at 1500rpm using exhaust gas recirculation.* International Journal of Hydrogen Energy, 28(8):901–908, 2003.
22. Einewall P, Tunestal P, and Johansson B. *Lean burn natural gas operation vs. stoichiometric operation with EGR and a three way catalyst.* Technical report, SAE Technical Paper,2005.
23. Smith JA and Bartley GJ. *Stoichiometric operation of a gas engine utilizing synthesis gas and EGR for NO_x control.* J. Eng. Gas Turbines Power, 122(4):617–623, 2000.
24. Saanum I, Bysveen M, Tunestal P, and Johansson B. *Lean burn versus stoichiometric operation with egr and 3-way catalyst of an engine fueled with natural gas and hydrogen enriched natural gas.* SAE Transactions, pages 35- 45, 2007.
25. Verhelst S, Demuynck J, Martin S, Vermeir M, and Sierens R. *Investigation of supercharging strategies for PFI hydrogen engines.* Technical report, SAE Technical Paper, 2010.
26. Tsujimura T and Suzuki Y. *Development of a large-sized direct injection hydrogen engine for a stationary power generator.* International Journal of Hydrogen Energy, 44(22):11355–11369, 2019.
27. Bardis K, Kyrtatos P, Xu G, Barro C, Wright YM, and Boulouchos K. *Development and validation of a novel quasi-dimensional combustion model for un-scavenged prechamber gas engines with numerical simulations and engine experiments.* International Journal of Engine Research, page 1468087420951338, 2020.
28. Lämmle C. *Numerical and experimental study of flame propagation and knock in a compressed natural gas engine.* PhD thesis, ETH Zurich, 2005.
29. Goodwin DG and Moffat HK. *Cantera.* URL http://www.cantera.org/docs/sphinx/html/index, 2001.
30. Bates L, Bradley D, Paczko G, and Peters N. *Engine hot spots: Modes of auto-ignition and reaction propagation.* Combustion and Flame, 166:80–85, 2016.
31. Li T, Yin T, and Wang B. *A phenomenological model of knock intensity in spark-ignition engines.* Energy Conversion and Management, 148:1233–1247, 2017.

32. Kalghatgi G, Algunaibet I, and Morganti K. *On knock intensity and super-knock in SI engines.* SAE International Journal of Engines, 10(3):1051–1063, 2017. 33. Pierre Boivin. Reduced-kinetic mechanisms for hydrogen and syngas combustion including autoignition. 2011.

33. Krisman A, Hawkes ER, and Chen JH. *The structure and propagation of laminar flames under autoignitive conditions.* Combustion and Flame, 188:399–411, 2018.

34. Gong X and Ren Z. *Flame speed scaling in autoignition-assisted freely propagating n-heptane/air flames.* Proceedings of the Combustion Institute, 38(2):2153–2161, 2021.

35. Puduppakkam KV, Modak AU, Wang C, Hodgson D, Naik CV, and Meeks E. *Generating laminar flame speed libraries for autoignition conditions.* In Turbo Expo: Power for Land, Sea, and Air, volume 84133, page V04BT04A004. American Society of Mechanical Engineers, 2020.

36. Bardis K, Kyrtatos P, Barro C, Denisov A, Wright YM, Herrmann K, and Boulouchos K. *A novel one-and zero-dimensional model for turbulent jet ignition.* Flow, Turbulence and Combustion, pages 1–36, 2021.

37. Biswas S, Tanvir S, Wang H, and Qiao L. *On ignition mechanisms of premixed CH4/air and H2/air using a hot turbulent jet generated by pre-chamber combustion.* Applied Thermal Engineering, 106:925–937, 2016

38. Bardis K, Xu G, Kyrtatos P, Wright YM, and Boulouchos K. *A zero dimensional turbulence and heat transfer phenomenological model for prechamber gas engines.* SAE Technical Paper No. 2018-01-1453, 2018

10 Appendix

Minutes

Workshop on Hydrogen Internal Combustion Engines, August 19, 2021

(online meeting via Zoom with 18 participants from Swiss Academia and Industry)

On the occasion of a computational project on hydrogen (H2) for Internal Combustion Engines (ICE), funded by BFE and carried out in LAV/ETH Zurich between September 2020 and June 2021, an online workshop has taken place with the participation of Swiss Academic groups (denoted with Fi) and Swiss industrial companies (denoted with Ii) and coordinated by the BFE grant manager Mr. Stephan Renz and program leader Dr. Carina Ales.

Content/Statements/Presentation:

Following a brief introduction on the scope of the event by Mr. Stephan Renz, partners have offered their statements on related work, either existing or planned, concerning H2-combustion in IC engines.

- F1 declared their interest in investigating fundamental issues of H2 combustion in an optically accessible engine-like test-rig and application oriented investigations in a single cylinder engine.

- F2 described both past work on H2/CH4 admixtures as engine fuels and a new project, starting with funding from BFE on direct injection (DI)-stratified engine combustion of H2, in cooperation with a German University.
- F3 presented a project idea with support from an industrial partner, and in the interest of a local public transportation authority, which deals with the development and implementation of multicylinder engine in a bus using H2 in lean or stoichiometric operation with EGR.
- F4, I1, I2, I3 referred to application in fuel cells, closed cycle H2 engines, simulation models and interest in the development of virtual sensors.

Presentation of H2 IC engine project at LAV/ETH-Zurich (F5):

The presentation was given by Dr. K. Bardis who has been the responsible scientist/engineer for this project. The scope was to computationally investigate the relative performance of lean burn operation and compare it against the lambda=1+EGR combustion mode for a 20-cylinder engine operating with pure hydrogen as fuel for CHP application. The focus was set on steady state operation, at a constant engine speed of 1500 rpm and maximum load (corresponding to a BMEP of 17 bar) which is the typical operation point of such engines. The study employed a phenomenological 0-D combustion model for CH4 and H2 fuels, which was developed by Dr. K. Bardis on the framework of this project, as well as during his doctoral thesis. The model was integrated in the 1-D GT-Power modelling platform such that the connection with the turbocharger and the gas dynamics can be accounted for. A baseline GT-Power model for a lean-burn methane engine as well as the corresponding experimental data for a single operating point were made available by an industrial company. Results/outcomes of the work are included in the final BFE-report of ETH-Zurich which will be published on www.aramis.admin.ch.

After the model validation has been carried out for the lean-burn engine operating with methane, comparative investigations of lean-burn against lambda=1+EGR were performed for methane and hydrogen fuels. Various performance criteria were included; namely, the thermodynamic efficiency, the NOx emissions, the knocking propensity, the maximum cylinder pressure and the gas temperature before the turbine. A disclaimer was been made that the simulation results of the study are indicative of the relative trends that are expected with H2 as fuel, but no precise quantitative predictions can be made in view of the absence of experimental verification.

The major outcomes of the simulation study are in summary the following:

- The thermodynamic efficiency of the engine operated with H2 is similar to the one operated with CH4.
- The pre-chamber ignition concept yields for both fuels and both operating modes slight performance advantage under NOx limited operation.
- The maximum achievable efficiency is higher for the lean-burn concept vs. the lambda=1+EGR under unconstrained NOx operation. If, however, the legislated NOx limit of 100 mg/Nm3 at 5% O2 is taken into account, which is more representative of the actual conditions, the attainable efficiency of the two modes is similar, since the lean operation requires a delayed spark timing to respect the NOx emissions limit.
- Overall, in the case of H2 engine with port fuel injection, the lean burn concept requires very high pressure ratios over the compressor and, therefore, possibly two stage turbocharger for achieving high BMEP levels, and may faces difficulty in achieving very low NOx-emissions according to current and future emission legislations.
- On the other hand, the lambda=1+EGR concept suffers from relatively high heat loads on critical components and may, in particular, approach the gas temperature limit in the turbine inlet.

It is worth mentioning that the obtained results for hydrogen operation apply for port fuel injection and a fixed compression ratio. A potential application of direct injection and parametric variation of the compression ratio may yield further advantages in terms of power density and differences in the relative trends.

Q&A session/feedback/discussion:

Mr. Stephan Renz thereafter moderated the Q&A session, having initiated the discussion with critical reflection on the presentation, soliciting feedback from the meeting participants. Examples from the inputs are given below:

Research institutes (Fi):

- In addition to knocking (end gas autoignition), hot surface ignition may be a strict limiting factor for the attainable efficiency of the H2 IC engines. In particular for lambda=1+EGR this may be particularly important.
- Investigation of hot surface ignition can be carried out in an optically accessible engine-like test-rig.
- First experience with H2 admixtures yielded very positive results. In particular the compression ratio can be increased ("Diesel-like") with high thermodynamic efficiency.
- For both fuels the issue of combustion stability at the flammability limits is important and can be assessed only by experimental investigations.

Industry companies (Ii):

- Lean H2 operation is considered easier and less complex solution, therefore, it is given priority for industrial application in comparison to the lambda=1+EGR concept.
- The question of minimal NOx-emissions is related to the feasibility of H2-SCR aftertreatment with lower light-of temperature.
- In steady state operation the lean burn concept has been shown to produce low NOx emission; however, under transient conditions, control schemes may prove to be very complex.
- Also with lambda=1+EGR, engine control under transient conditions for stoichiometric catalysts is seen as a major challenge.
- Overall, industrial companies recognized the potential of the lambda=1+EGR concept and show a certain interest, even if it is rather "complex" to start with.

Conclusion/Outlook:

A consensus has resulted on the meaningfulness of H2-combustion in IC engines as a cost effective route to decarbonization and several research questions have been identified, which will be investigated in future projects. Finally Mr. S. Renz, Dr. C. Alles and Dr. K. Bardis expressed their sincere gratitude to the Swiss Industry and Academia for the fruitful discussion and useful feedback.

K. Bardis, LAV ETHZ, 15.09.2021